Numerical Simulation of Hygrothermomechanical Deformations of Bituminous Pavements in the City of Ouagadougou Subjected to Tropical Dry Showers

Sidpouita Mathilde Koudougou, Konfe Amadou, David y K Toguyeni, Anne Pantet, Tariq Ouahbi

Current Journal of Applied Science and Technology

41(36): 19-37, 2022; Article no.CJAST.91284
ISSN: 2457-1024
(Past name: British Journal of Applied Science & Technology, Past ISSN: 2231-0843, NLM ID: 101664541)

Numerical Simulation of Hygrothermomechanical Deformations of Bituminous Pavements in the City of Ouagadougou Subjected to Tropical Dry Showers

Sidpouita Mathilde Koudougou [a,b*], Konfe Amadou [c], David Yemboini Kader Toguyeni [a,b], Anne Pantet [d] and Tariq Ouahbi [d]

[a] Institut du Génie des Systèmes Industriels et Textiles, Ecole Polytechnique de Ouagadougou, Ouagadougou, Burkina Faso.
[b] Laboratoire de Physique et de Chimie de l'Environnement, Ouagadougou, Burkina Faso.
[c] Laboratoire d'énergies Thermiques Renouvelables, Ouagadougou, Burkina Faso.
[d] Laboratoire Ondes et Milieux Complexes, UMR 6294, Le Havre, France.

Authors' contributions

This work was carried out in collaboration among all authors. All authors read and approved the final manuscript.

Article Information

DOI: 10.9734/CJAST/2022/v41i363964

Open Peer Review History:
This journal follows the Advanced Open Peer Review policy. Identity of the Reviewers, Editor(s) and additional Reviewers, peer review comments, different versions of the manuscript, comments of the editors, etc are available here: https://www.sdiarticle5.com/review-history/91284

Original Research Article

Received 02 August 2022
Accepted 08 October 2022
Published 18 October 2022

ABSTRACT

The waters of the torrential rains in the city of Ouagadougou lead to the appearance or amplification of damage to the surface of asphalt pavements during the rainy season. Road infrastructure maintenance campaigns follow one another almost every rainy season to fill potholes and cracks observed on the pavements. Several hypotheses can be put forward as to the origin of the action of water on the surface of pavements: the pressure of runoff water, infiltration, thermal expansion during the rainy episode, etc. These various reasons reveal the need to take rainwater into account when designing pavements. A previous study on the effect of heat waves on pavement design made some recommendations for better design. It has raised the interest to observe the impact of rain on pavement deformability.

The objective of this article is to estimate, as a first approach, the effect of tropical rains on the Thermomechanical behaviour of bituminous pavements formulated with pure grade 35/50 bitumen and grade 10/65 modified bitumen without trafic.

The properties of the road materials and the data from the statistical treatment of rainfall in the city

**Corresponding author: E-mail: koudougoumathilde@yahoo.fr;*

of Ouagadougou were determined. The software based on the finite element method was used to model the phenomena coupling the meteorological conditions to the mechanical structure of the pavement for the quantification of hygrothermal and mechanical deformations.
The bituminous pavements studied were subjected to maximum rainfall intensities of 53.06 mm/h, and 99 mm/h with respective frequencies of occurrence of 2 years and 15 years.
The comparison of the temperature profiles at the surface of the studied pavements, allowed to highlight the viscous character of the asphalt subjected (35/50 bitumen and grade 10/65 modified bitumen) to the rains of maximum intensity of 99 mm/h. The maximum deformations simulated during these rains are about 1.2 times greater in the wearing course than in the base course, which does not disrupt the classical order of temperature evolution in the different pavement layers under dry tropical conditions. These deformations obtained also respect the admissibility criteria in terms of pavement design for T2 trafic (151 to 300 Heavy Truck/day). This study could be expanded to include the permeability of bituminous surfaces and runoff phenomena that could provide information on the origin of the observed deterioration.

Keywords: Pavement; hygrothermomechanical; modeling; dry tropical weather.

1. INTRODUCTION

Hygrothermal modeling transfers appears in the literature as a special case of thermal transfers in pavements. However, heat transfer in pavements depends on weather conditions, including precipitation, because it is part of them.

To our knowledge, researchers studying heat transfer in pavements do not always include precipitation in the weather conditions. Taking precipitation into account would allow all meteorological conditions to be considered for the prediction of pavement temperature. The modelling of hygrothermal transfers makes it possible to propose to pavement design engineer's calculation tools that increase the accuracy of temperature prediction for a more rigorous pavement design [1].

Two approaches are used to evaluate the action of water on pavement temperature. In the first approach, researchers assume that the flow of the water film from precipitation is instantaneous and that there is no accumulation of rain on the pavement surface [1,2].

In a second approach, others try to study the transfer mechanisms during precipitation [3-5].

Yavuzturk et al. [1] developed a two-dimensional numerical model based on the finite difference method to predict temperature fluctuations at different depths and lateral locations in bituminous pavements. This model is unique in that it accounts for the energy flux from precipitation in the energy balance at the pavement surface. Hourly temperatures at any arbitrary point on a bituminous pavement are obtained by taking into account weather conditions, pavement geometry and orientation. In 2005, Yavuzturk et al. [1] improved the model by additionally evaluating the thermal deformations associated with these thermal fluctuations. Su Subsequently, [1] refined the model of [2] by studying the thermal deformations related to the orientation of the pavement surface slope and the precipitations in the different layers. This model showed that precipitation and evaporation have a significant cooling effect on pavement surface temperatures and that thermal stresses on asphalt pavements are strongly impacted by the thermal conductivity of the asphalt layers and their location in the pavement structure. They also demonstrated that the pavement slope angle can have a significant impact on the pavement temperature distribution. Depending on the surface, azimuth, temperatures on a sloped surface will be seasonally higher or lower than temperatures on a horizontal surface.

Heat transfer mechanisms over pavements during precipitation are poorly understood due to difficulties in capturing the many important physical processes and parameters in experiments and models.

Van buren et al, Cohard et al. [3,4] proposed heat transfer models including all surface energy balances to calculate soil surface temperature during precipitation and estimated runoff temperature as a function of precipitation and pavement surface temperature.
Similarly, Janke et al. [4] suggested a more comprehensive model solving a one-dimensional

(1D) runoff model numerically coupled with a 1D heat balance for the subsurface and runoff.

Kertesz and Sansalone [6] used field measurements performed on asphalt pavements in conjunction with a heat balance model that combines the models used in the studies of Van buren et al., Janker et al., Herb et al., Kim et al., Sansalone and Teng, Thompson et al. 2008 [3,4,7-10] to investigate the transfer of thermal energy in the pavement during rainstorms.

In the previously cited studies, the runoff is in an equilibrium state with the surface (no vertical temperature gradient was assumed in the runoff) and no infiltration was allowed. They do not take into account the dynamics of the flows, more precisely the equations of the flows taking place according to the depth and the speeds of runoff.

Omidvar et al. [11] developed a detailed two-dimensional model of heat and water transfer processes in impermeable bituminous pavement. This dynamic model of runoff along the vertical, showed that the temperature difference between the pavement surface and the runoff water can be larger or smaller for wide pavements and short duration precipitation (because the thickness of the runoff water downstream is greater than upstream). The model also indicated that the driving heat transfer processes for the runoff layer are heat gain from the pavement surface and heat loss from the net cooler precipitation flow and the warm runoff flow. Cooling by latent heat from the pavement was a secondary but not insignificant factor, while net radiation and sensible heat flux were insignificant under realistic, cloudy rainfall conditions.

The effects of water on the durability of concrete pavements are being increasingly studied [12-14].

For example, the results of the work of Mateos et al. [15] have challenged the validity of a number of assumptions adopted in the current mechanistic-empirical design procedures for concrete pavements in California.

If the study of water action on concrete pavements is current in developed countries, in the area where pavements are still constructed with asphalt, this study is necessary for a better design. The asphalt pavement surfaces in the city of Ouagadougou are formulated with draining asphalt. This type of asphalt is designed to deliberately allow water to penetrate the pavement in order to limit vehicle splashing and to limit the noise produced by the tires and the pavement. With the exception of this planned acceptance of water into the pavement, water is generally undesirable because it often causes stripping of the asphalt, with separation of the aggregate and binder.

The action of water on the appearance or amplification of deterioration can be observed on asphalt pavements in dry tropical Africa, particularly during the rainy season. Road infrastructure maintenance campaigns follow one another almost year after year in the dry season to fill potholes and cracks observed on the pavements of the city of Ouagadougou. It is in this context that this study of hygrothermal transfer phenomena in the bituminous pavements of the city of Ouagadougou was undertaken. It aims at evaluating the impact of thermomechanical deformations induced by rainfall on pavement design. The hygrothermal deformations of the pavements of the NR1 and NR2 national roads of the city of Ouagadougou were numerically quantified using the Comsol Multiphysics software.

The thermomechanical deformations that will be quantified will be compared to the permissible deformations proposed by the practical guide for the design of tropical pavements in order to estimate the unique effect of rain on the deterioration condition of new asphalt pavements.

2. MATERIALS AND METHODS

2.1 Materials

Within the framework of this work, the national roads 1 and 2 of the city of Ouagadougou, were studied. These are the sections located between kilometric points KP2+675 and KP2+850, with a length of 175 meters for the NR4 (national road 4) ; and kilometric points PK00 and PK00+275, with a length of 275 meters for the NR2 (national road 2). The NR4 is located to the west of the city and can be identified by the following geographical coordinates N 12.34359°, W 001.56948°. The NR2 is located to the north of the city of Ouagadougou with the following geographical coordinates N 12.38836°, W 001.48810°. From a geotechnical point of view, both pavements are flexible and made up of four (4) layers: a wearing course and a base course in bituminous mix, a sub-base course above the subgrade soil.

The different materials of the pavement layers were reconstituted in the laboratory from the formulas used by road builders.

2.1.1 Bitumen

Pure 50/70, 35/50 and modified 10/65 bitumens were used in the design of the surface courses. The characteristics of these bitumens are listed in Table 1.

2.1.2 Asphalt concrete layers

The asphalt mixes used in the wearing course and the base course are composed of a mixture of crushed granite and bitumen. The granites used for the asphalt mixes of the two pavements come from different quarries. The granites for the NR4 are from the Yimdi quarry, located at N 12.30098°, W 001.69862° and those for the NR2, from the Yagma quarry, located at N 12.38555°, W 001.55814°.

The formulas of the asphalt layers, coming from the data of the road builders, are arranged in the tables (Table 2 and Table 3).

2.1.3 Sub-base course and soil subgrade

The subgrade is obtained by lithostabilization [16].

The Lithostab (LITHO) used in this work is a mixture of 30% crushed granites and lateritic clayey gravels (LGC) from Yimdi at N 12.31131°, W 001.65680° for NR4 and from Banogo at 12° 18' 14" for NR2. The subgrade is exclusively composed of the same gravelly clayey lateritic material.

The geotechnical properties are recorded in Table 4.

Table 1. Bitumen identification

Layer	Bitumen grade	ρ (kg/m^3)	Penetrability (°C)	BRT (°C)
AC and BC NR4	35/50	1.025	38.66	54.75
AC-NR2	10/65	1.026	27.16	65.5
BC- NR2	35/50	1.018	37.83	54.25

Table 2. Composition of asphalt mixes for the NR4

Asphalt Concrete (AC)		Grave Bitumen (BC)	
Components	**Dosage (%)**	**Components**	**Dosage (%)**
6/10	43.3	10/14	33
4/6	16.5	6/10	13
0/4	34	4/10	14.8
Bitumen 35/50	5.2	0/4	34
		Bitumen 35/50	4.2

Table 3. Composition of asphalt mixes for the NR2

Asphalt Concrete (AC)		Grave Bitumen (BC)	
Components	**Dosage (%)**	**Components**	**Dosage (%)**
6/10	38.69	10/14	28.7
4/6	15.86	4/10	20
0/4	45.45	0/4	45
Bitumen 10/65	5.4	Bitumen 35/50	4.3

Table 4. Geotechnical characteristics of the LITHO and LGC

Mixes Identification		Size distribution (%)			Plasticity index I_P (%)	Optimum Modified Proctor		I_{CBR} at 95% OPM
		0.08 mm	2 mm	10 mm		w_{OPM} (%)	ρd (g/cm^3)	
NR4	LITHO	16	32	70	15	7.3	2.24	68
NR4	LGC	19	36	86	16	7.1	2.15	49
NR2	LITHO	24.5	48.5	87.5	13	9.4	2.12	68
NR2	LGC	18	40	79	14	7.4	2.15	41.5

2.2 Methods

The work carried out in this article was carried out in three steps corresponding to the mathematical formulation of the problem, the determination of the parameters (geotechnical and thermophysical meteorological) necessary for the implementation followed by the numerical simulation using the Comsol Multiphysics 5.2 software (Fig.1.).

Most of the geotechnical and thermophysical parameters were obtained after a laboratory reconstruction of the pavement layers.

2.2.1 Statistical analysis of rainfall data

The first data on rainfall provided by the meteorological services of Burkina Faso is the height of water falling per day, the sum of the heights collected in 24 hours (from 6:00 a.m. UTC on the day to 6:00 a.m. the next day). This data does not allow us to determine the number associated with the duration of the rain. For this purpose, the most unfavorable quantifiable rainfall hypothesis is made. It is assumed that the daily amount of water obtained from the meteorological services is associated with a single shower of 3 hours' duration.

According to the work of Bourier [17], when rainfall records are available (duration of the shower, height of water fallen), the average intensity of each rainfall can be known, which is generally acceptable for short duration showers but quite random for long duration rainfall. For a given time interval, the synthetic hyetogram was determined by Talbot's homographic formula because it is adapted for rainfall intensities of less than 24 hours:

$$i(t) = \frac{a(T_r)}{t+b(T_r)} \quad (1)$$

$a(T_r)$, $b(T_r)$ are the Montana coefficients by linear regression of $\ln(i(t))$ for the return frequency T_r.

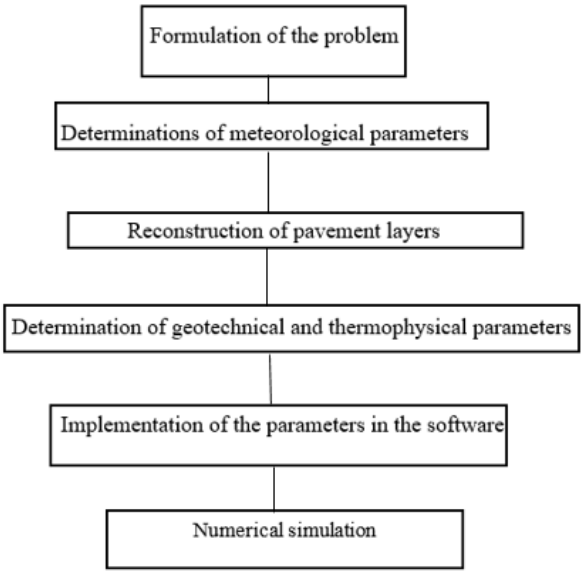

Fig. 1. Schematic representation of the methodoly

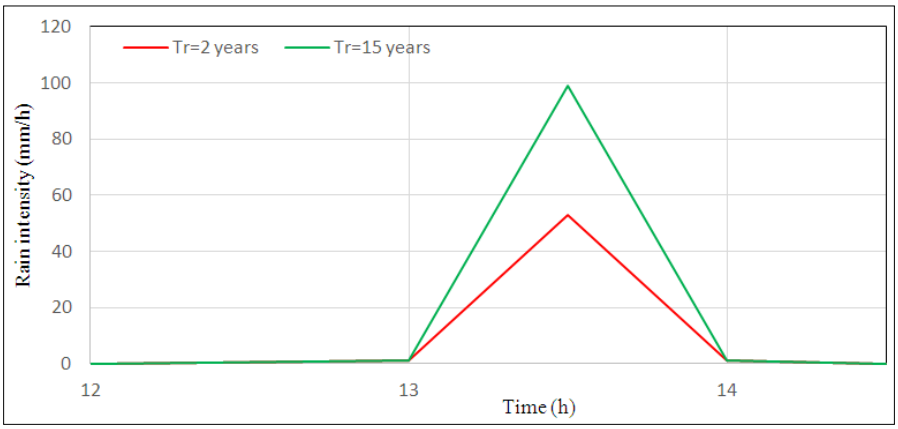

Fig. 2. Intensity profile was then defined from the desbordes project rainfall model [18]

The intensity profile was then defined from the Desbordes project rainfall model [18] adapted to African tropical rains according to the work of [19] whose duration is less than or equal to 3 hours (Fig. 2).

2.2.2 Numerical model

When the pavement is subjected to a rainfall event, additional energy is added to the energy available at the pavement/atmosphere interface (Fig. 3). These are the energy induced by the rainwater falling on the pavement and the energy related to the evaporation of the water present on the pavement surface.Furthermore, it is assumed that drainage occurs instantaneously in a laminar flow and that infiltration and runoff phenomena are not taken into account in the model. The heat transfer in the different layers of the pavement is therefore governed by the radiative energies exchanged between the surface and the atmosphere and the energies previously described: the absorbed energy, the energy emitted by the surface towards the sky, the energy induced by the rainfall, the energy produced by the evaporation of a thin film of water available on the surface. The pavement is often considered in the literature as a semi-infinite, isotropic, linear, low-temperature viscoelastic, water-impermeable homogeneous solid medium [20]. It is not expected to produce energy translated into zero internal heat flux (zero geothermal gradient) [21]. It is subject to local weather conditions. The assumption of perfect contact between layers results in temperature continuity and heat flux conservation at the interfaces between two successive layers in the linear thermoelastic model with a rainwater film.

The proposed linear thermoelastic numerical model can be represented schematically as shown in Fig. 3.

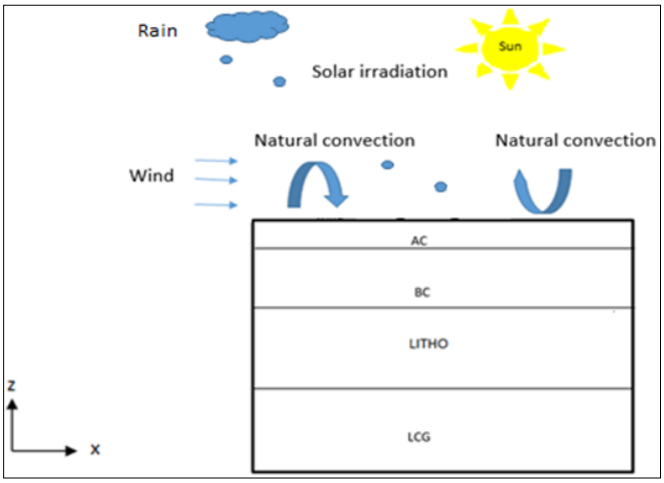

Fig. 3. linear thermoelastic numerical model with rain

2.2.2.1 The mathematical formulation of the problem

The physical problem posed in this article is a thermal problem leading to a mechanical behaviour.

2.2.2.1.1 Formulation of heat transfer phenomena

The equation governing the heat transfer in the different layers of the pavement is given by :

$$\Delta T = \frac{1}{D}\frac{\partial T}{\partial t} \quad (2)$$

Energy balance in the pavement: The pavement is subject to weather and trafic conditions. Under these conditions, the net energy φ_{net} (W/m^2) available at its surface which is then transferred by conduction to the different layers is given by the following relation [22] :

$$\varphi_{net} = \varphi_a + \varphi_r + \varphi_{cond} \pm \varphi_{conv} + \varphi_{rain} + \varphi_e \quad (3)$$

φ_a : energy absorbed by the pavement from direct solar radiation
φ_r : energy emitted from the pavement to the sky
φ_{cond} : energy transferred to the pavement by conduction
φ_{conv} : energy transferred to the pavement by convection
φ_{rain} : energy taken by rainfall
φ_e : energy extracted from rainwater evaporation

Heat flux absorbed by the pavement:

There are two components to solar radiation incident on the pavement surface :
The sun emits short-wave radiation onto the pavement surface. Part of its energy is absorbed by the pavement surface causing a rise in the pavement temperature. This energy is given by :

$\varphi_a = (1-\alpha)R_g$ Where α is the albedo and R_g the global radiation (4)

In our case, the albedo of the road surface is equal to 0.18 [20].

The pavement in turn emits long wave radiation to the sky according to the Stefan-Boltzmann law :

$$\varphi_r = \sigma\epsilon\left(T^4_{sky} - T^4_s\right) \quad (5)$$

with σ is the Boltzmann constant, ϵ the emissivity of the pavement surface, T_{sky} , sky temperature , T_s the temperature at the surface of the pavement, ϵ The emissivity of the pavement surface is taken equal to 0,92 [17] ;

The sky temperature is given by [23] :

$$T_{sky} = 94.12\ln(P_v) - 13\ I_c + 0.314T_{air} \quad (6)$$

where P_v is the vapor pressure, I_c is the sky clarity index and T_{air} is the air temperature

Heat flux transmitted to the pavement by conduction: The energy flow obtained by conduction φ_{cond} at the pavement surface can be approximately calculated by the following relationship [24] :

$$\varphi_{cond} = -k\frac{T_z - T_s}{z} \quad (7)$$

with k the thermal conductivity of the layer, T_z the temperature at depth z

Heat flow generated by convection phenomena: Natural convection is a transfer of energy between the air and the pavement surface.

The convective energy is given by Newton's law :

$$\varphi_{conv} = h_c(T_s - T_{air}) \quad (8)$$

With h_c the convective exchange coefficient

The wind speed, V_{wind} of the city of Ouagadougou, is generally below 5 m/s at 30 m from the ground [25], therefore the expression of the convective exchange coefficient [20,21] is the following.

$$h_c = 5.8 + 4.1 \times V_{wind} \quad (9)$$

Energy taken by rainfall: Rainfall causes energy to be deposited on the pavement surface. This energy is related to the intensity of the rain and the thermal gradient between the surface temperature and the rainwater. It is given by the following relation [2]:

$$\varphi_{rain} = 3{,}6 \times 10^{-6} \times i \times \rho_{water} \times C_{pwater}\,(T_{rain} - T_s) \quad (10)$$

i is the intensity of the rain; ρ_{water} the density of the water; $C_{p_{water}}$ thermal capacity of water; T_{rain} the temperature of the rainwater.

Energy extracted from rainwater evaporation: Rainwater droplets that hit the surface of the pavement form a sheet of water that can evaporate or run off. The evaporation of the water causes the pavement to cool. The energy produced by the evaporation mechanism is given by the following relationship [1,2]:

$$\varphi_e = h_{fg} \times \dot{m}_{water} \; C_{p_{water}} (HR_{air} - HR_s) \qquad (11)$$

h_{fg} is the latent heat of vaporization, HR_{air} the relative humidity of the ambient air, HR_s the humidity of the saturated air on the surface of the pavement. The values of $\dot{m}_{eau}$, HR_s were determined using empirical value tables [26].

Strains: The thermal stresses induced by heat transfer are given the following relationship [27] :

$$\epsilon_T = \alpha_{th} \Delta T \qquad (12)$$

with α_{th} the coefficient of thermal expansion and ΔT the temperature variation at the surface of the layer

Linear thermoelastic model of pavement subjected to rain: Heat transfer phenomena are described by partial differential equations of the temperature associated with boundary conditions. Numerical methods are used to obtain approximate values of the temperature at discrete points called nodes. One such method is the finite element method (FEM) developed and applied to solve many heat transfer problems [28]. The FEM method requires the discretization of the problem domain into several subdomains for which the heat transfer problem is analyzed. Each subdomain is called a finite element, thus giving the method its name. The computed global field is then determined by a finite number of field values on the nodes [29]. The resolution with Comsol Multiphysics 5.2 software consists in studying the thermomechanical response of the pavement under thermohydric loading. It goes through the following steps of defining the pavement geometry, meshing the pavement, defining the physical properties of the materials and the boundary conditions, numerical resolution and analysis of the results (post-processing). The finite element approach allows to obtain a sufficiently accurate visualization of the pavement behaviour in two dimensions.

The numerical model is built on the finite element method using the Comsol Multiphysics software. The input data are the geometrical characteristics of the pavement, the thermophysical and geotechnical properties of the materials, the hourly evolution of the meteorological parameters as well as the braking parameters obtained from the mathematical formula of the problem.

The output parameters are the temperature, displacement and deformation fields associated with precise positions in the different layers of the pavement such as the surface of the wearing course, the interface between the wearing course and the base course, the middle of the sub-base and the subgrade soil.

The initial temperature condition: The initial condition chosen, was obtained by theoretical calculation [30] from the general solution of the heat equation (1) can take the following real form:

$$T(z,t) = \overline{T} + A\sin(\omega t - \varphi(z)) \text{ [31]} \qquad (13)$$

$A = A_0 e^{-kz}$ with A_0 is the daily temperature amplitude ; (14)

$\varphi = kz$ is the phase ; (15)

$$k = \sqrt{\frac{\pi}{D_T}} \qquad (16)$$

The results are reported in Table 5.

Meteorological and geometrical parameters of the model: The meteorological data used for the simulations come from the National Directorate of Meteorology of Burkina Faso.

Table 5. Determined initial temperatures of the different layers

$\overline{T}$ at 06:00 am	A_0	T_{BB}	T_{GB}	T_{LITHO}	T_{GAL}
23.8°C	19.5°C	21.1°C	15.7°C	15.6°C	15.6°C

Table 6. Summary table of thermo-physical and geotechnical pavements data.

	Pavement layer	e	E	ν	k	C_p	ρ	α_{th}
NR2	AC	5	$4.2266T^3 + 776.81T^2 - 47325T + 956663$	$0.15 + 0.35/(1 + \exp(3.1849 - 0.04233\,T(°F))$ a	1.747	900a	2310	2.10^{-5}c
	BC	12	$1.2248T^3 + 223.28T^2 - 13521T + 272697$	$0.15 + 0.35/(1 + \exp(3.1849 - 0.04233\,T(°F))$ a	1.566	900a	2330	2.10^{-5}c
	LITHO	20	4300×10^6	0.4_b	0.77	900b	2140	
	LGC	20	450×10^6	0.4_b	0.67	600b	2120	

a-[32] ; b-[21] ; c-[33,35]

Table 7. Summary table of thermo-physical and geotechnical pavements data

	Pavement layer	e	E	ν	k	C_p	ρ	α_{th}
NR4		cm	Pa		W /mK	J/kg /°C	kg /m^3	$\frac{\mu m}{m}$/°C
	AC	4	$-1018.1T^3 + 181094T^2 - 10^7$	$0.15 + 0.35/(1 + \exp(3.1849 - 0.04233\,T(°F))$ a	1.702	900a	2260	2.10^{-5}c
	BC	15	$-1181.1T^3 + 210294T^2 - 410^7$	$0.15 + 0.35/(1 + \exp(3.1849 - 0.04233\,T(°F))$ a	1.584	900a	2300	2.10^{-5}c
	LITHO	20	34×10^8	0.4_b	0.77	900b	2240	
	LGC	20	14.70×10^8	0.4_b	0.67	600b	2120	

a-[32] ; b-[21] ; c-[33,35]

These are hourly values from 6 am to 6 pm of solar radiation, air temperature, dew point temperature, air humidity, wind speed.

The numerical model constructed is two-dimensional. The results are obtained over the length and depth of the pavement.

Thermo-physical and geotechnical parameters of the model: He thermal conductivities of the four layers were measured while the other thermo-physical parameters such as the coefficient of thermal expansion [27] and the specific heat capacity were taken from the literature [32,33].

It should be noted that the stiffness moduli of asphalt concrete were obtained experimentally by compression tests according to the protocol described in the work of Koudougou et al [34].

The moduli of the foundation and subgrade layers are obtained by applying the empirical relations [21]. They are assumed to be temperature invariant.

The geotechnical and thermo-physical properties of the surface layers are listed in Tables 6 and 7.

3. RESULTS AND DISCUSSIONS

The model presented was simulated under extreme weather conditions. For this purpose, the hottest historical day of the year 2018, which corresponds to april 06, 2018 was chosen.

The rainy episode occurs at the time when the road surface is hottest, i.e. between 12pm and 2.30 [30].

3.1 Thermal Response of the Pavement During a Rain Event

The general pattern of simulated temperature profiles for different rainfall intensities indicates that temperatures decrease with increasing rainfall intensity (Fig. 2). This means that the induced latent and sensible heats would increase with rain intensity. This increase is induced by a cooling of the pavement, of a magnitude proportional to the intensity of the rainfall.

The temperature drop recorded on the surface of the pavements is about 4°C for a rain duration of 150 min on the surface. The work of Kim et al. [36] also presents a similar temperature drop and that of Wang et al. [37] evaluates the latter at 4.5°C for a 280 min rainfall at 2 cm from the pavement surface. This difference is related to the composition of the asphalt layer, the measurement thickness and the continental climatic conditions of the site.

The temperature profile (Fig. 4) at the surface of the roadway during rain is non-linear with respect to time, unlike the linear profile that would be obtained in the absence of rain [30].

Before the rain, the temperature profiles on the surface of the roadway, for rains with maximum intensities of 53.06 mm/h and 99 mm/h show for the two roads a difference of 0.86°C with a higher temperature for the NR4.

During rain, the surface layer of NR4 formulated with 35/50 pure bitumen cools less quickly with a difference of 0.02°C than the surface layer of NR2 formulated with 10/65 modified bitumen for an intensity maximum rainfall of 53.6 mm/h.

For a maximum rain intensity of 99 mm/h, the opposite effect with a difference of 0.03°C is observed on the road surface. This reveals the more viscous rheological character of the NR2 surface layer due to the 10/65 modified bitumen.

The proposed hygrothermal model therefore reveals that for rains with a maximum intensity of 53.6 mm/h, the rate of cooling is proportional to the rate of heating. For rains with a maximum intensity of 99 mm/h, it can be seen that the rate of cooling of the surface layer formulated with pure bitumen is greater than that formulated with modified bitumen.

In addition, the simulated maximum temperatures of 42.7°C and 43.4°C for NR2 and NR4 respectively (Fig. 4) are lower than the softening point temperatures of the different asphalts (Table 1).

The previous graphs show that for the duration of 2 hours and 30 min of rainfall, the order of the temperature profile in the different layers of the pavement is respected due to the long duration of the rainfall (Figs. 5.a, 5.b, 5.c, 5.d).

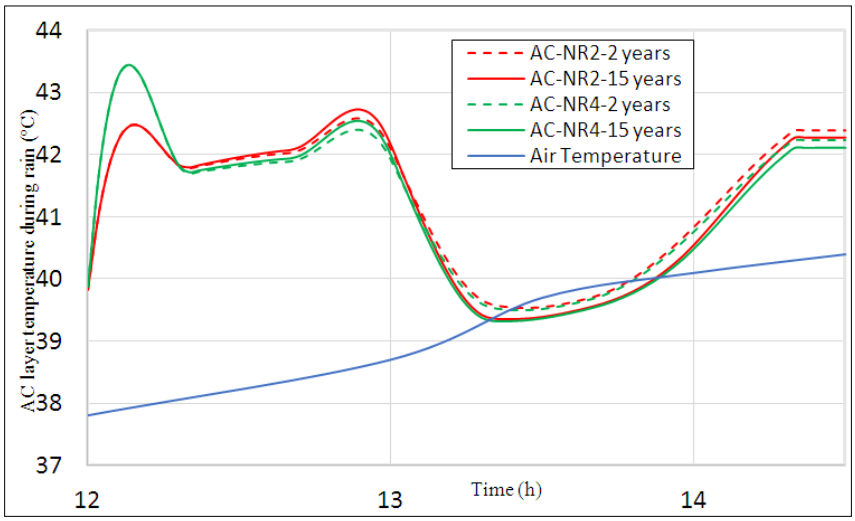

Fig. 4. Temperature profile at the pavement surface for 53.6 mm/h and 99 mm/h rainfall

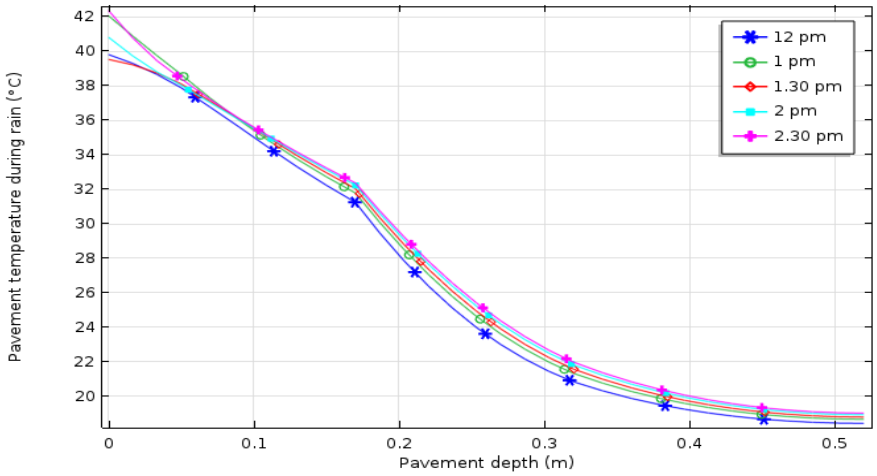

Fig. 5.a Temperature profile in the different layers of NR2 for a rainfall of maximum intensity of 53.6 mm/h

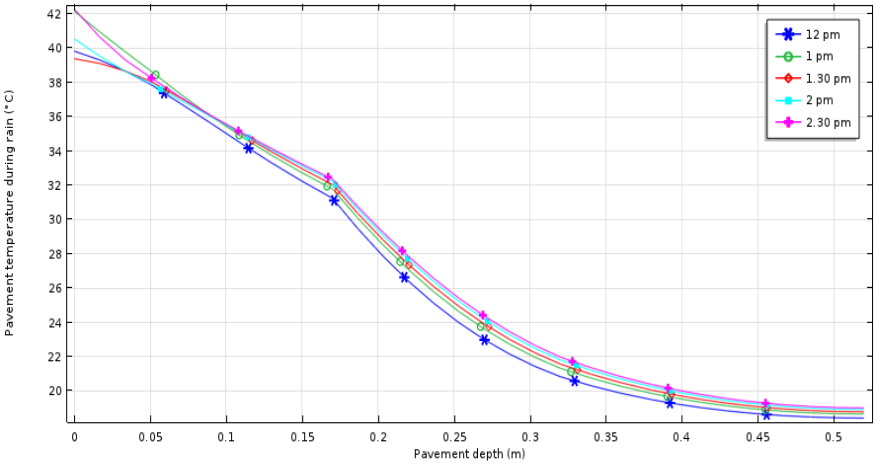

Fig. 5.b Temperature profile in the different layers of NR2 for a rainfall of maximum intensity of 99 mm/h

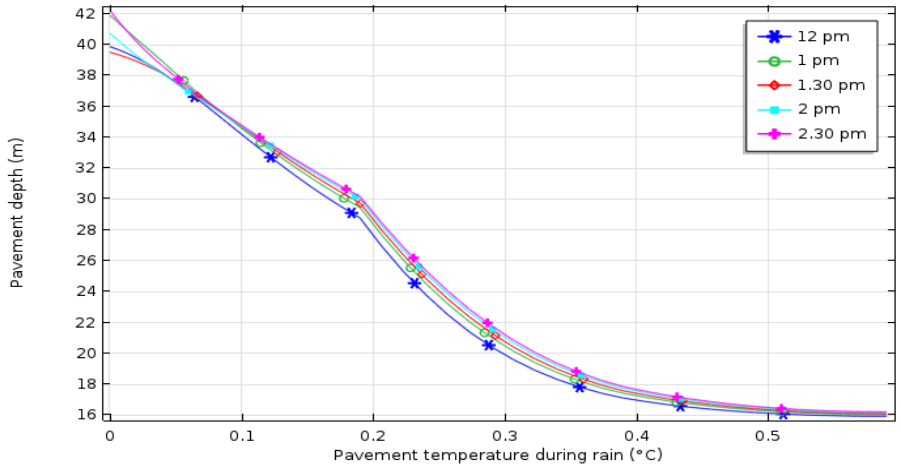

Fig. 5.c Temperature profile in the different layers of NR4 for a rainfall of maximum intensity of 53.6 mm/h

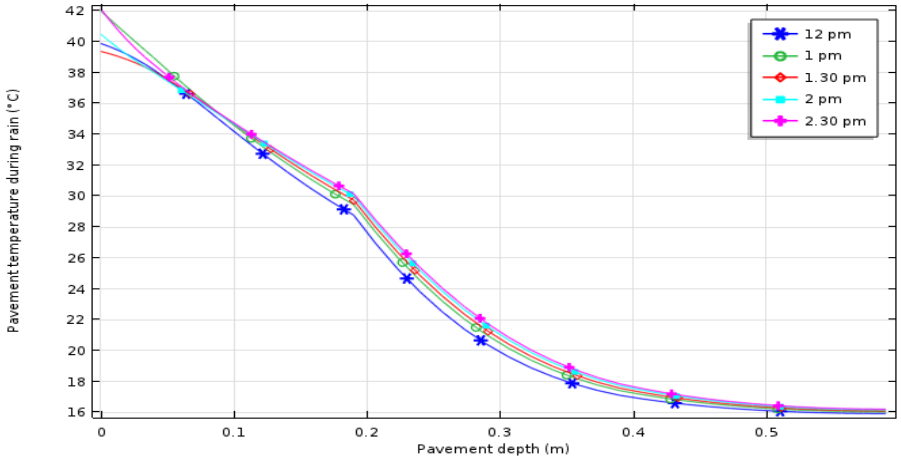

Fig. 5.d Temperature profile in the different layers of NR4 for a rainfall of maximum intensity of 99 mm/h

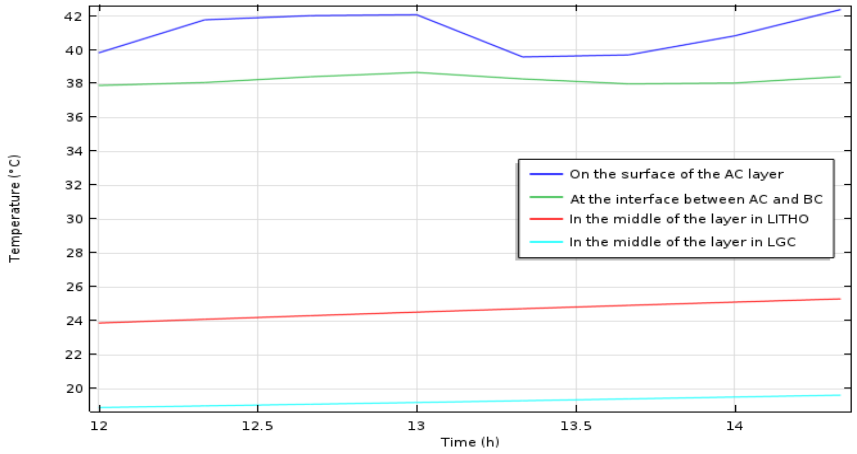

Fig. 6.a Evolution of the temperature in the different layers of the NR2 during the rainfall of maximum intensity of 53.6 mm/h

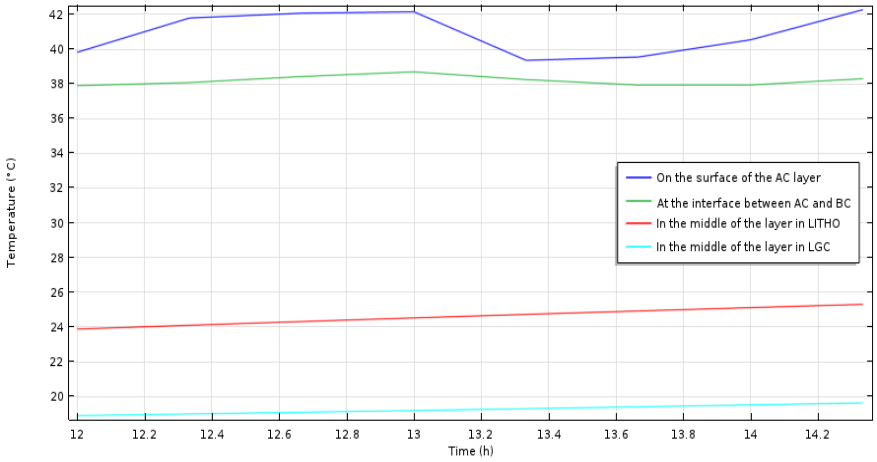

Fig. 6.b Temperature evolution in the different layers of NR2 during the maximum rainfall intensity of 99 mm/h

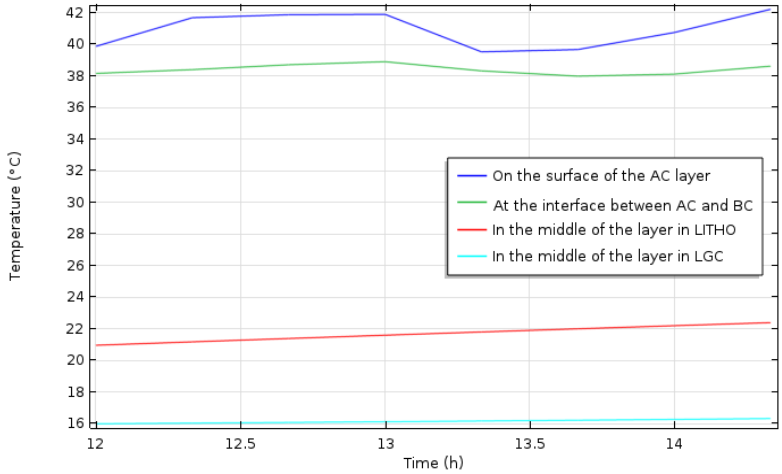

Fig. 6.c Evolution of the temperature in the different layers of the NR4 during the rainfall of maximum intensity of 53.6 mm/h

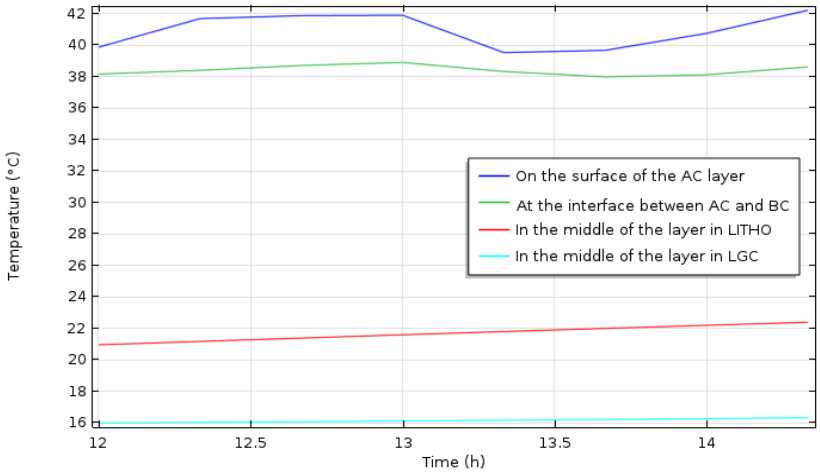

Fig. 6.d Evolution of the temperature in the different layers of the NR4 during the rainfall of maximum intensity of 53.6 mm/h

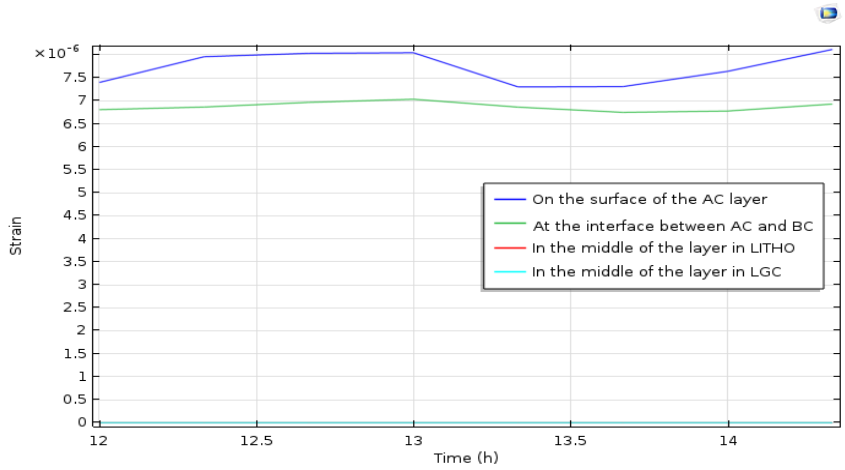

Fig. 7.a Temporal distribution of deformations according to depth in the different layers of NR2 during a rainfall of maximum intensity of 53.06 mm/h

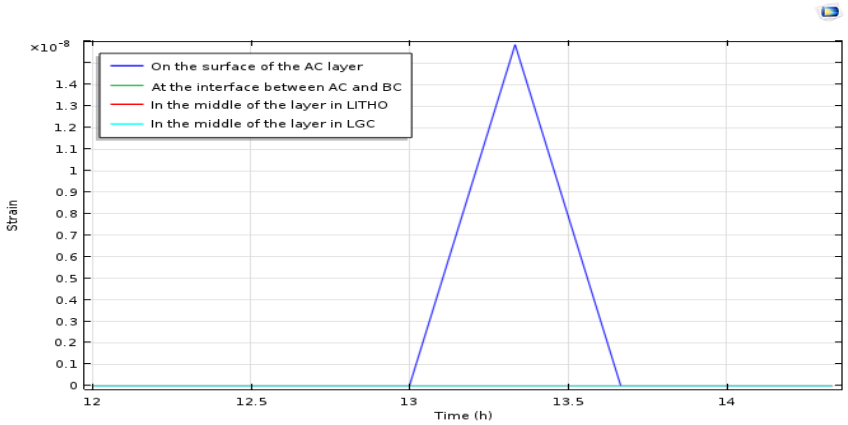

Fig. 7.b Temporal distribution of longitudinal deformations in the different layers of NR2 during a rainfall of maximum intensity of 53.06 mm/h

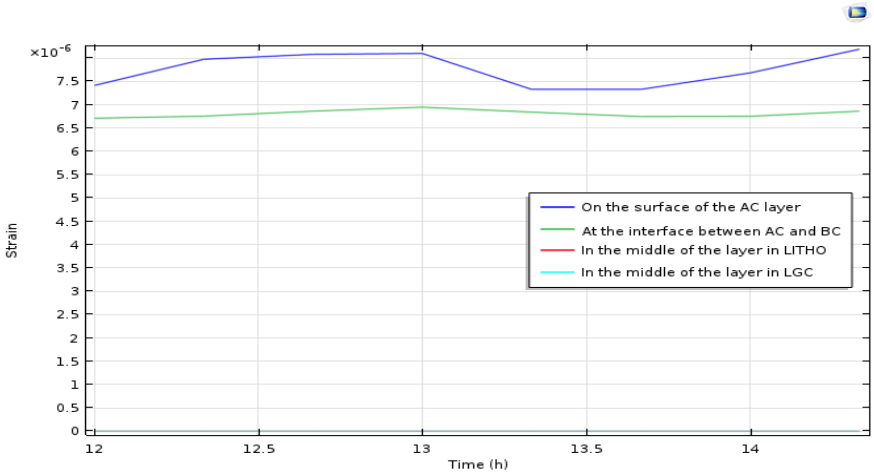

Fig. 7.c Temporal distribution of deformations according to depth in the different layers of NR2 during a rainfall of maximum intensity of 99 mm/h

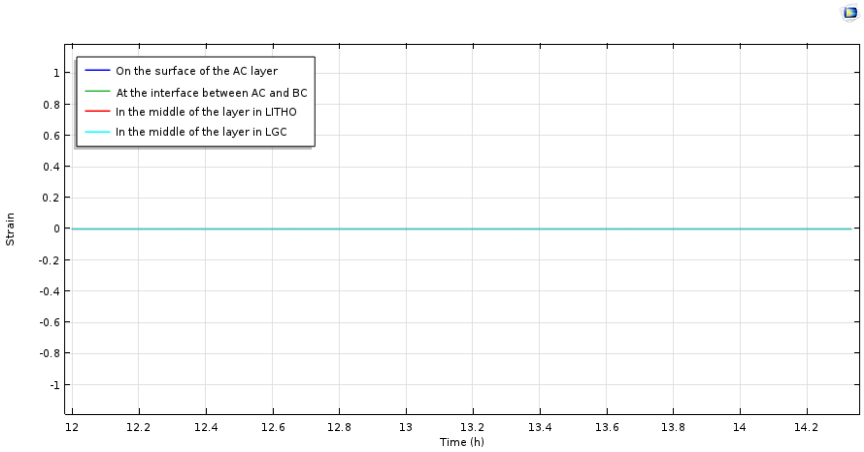

Fig. 7.d Temporal distribution of longitudinal deformations in the different layers of NR2 during a rainfall of maximum intensity of 99 mm/h

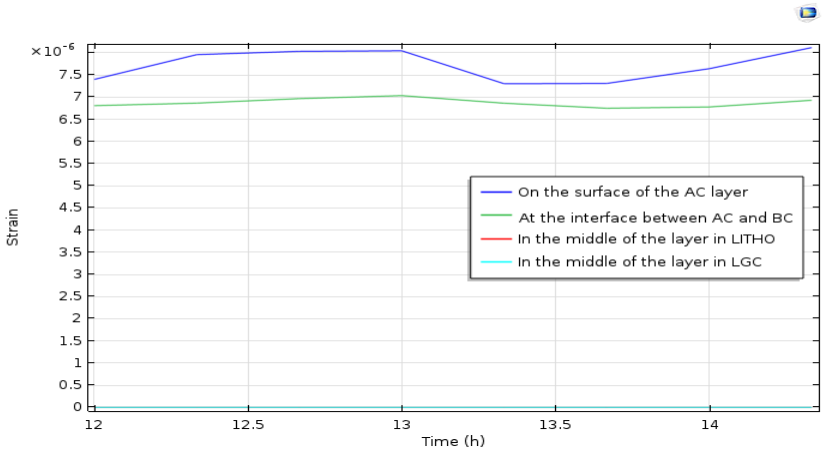

Fig. 8.a Temporal distribution of deformations according to depth in the different layers of NR4 during a rainfall of maximum intensity of 53.06 mm/h

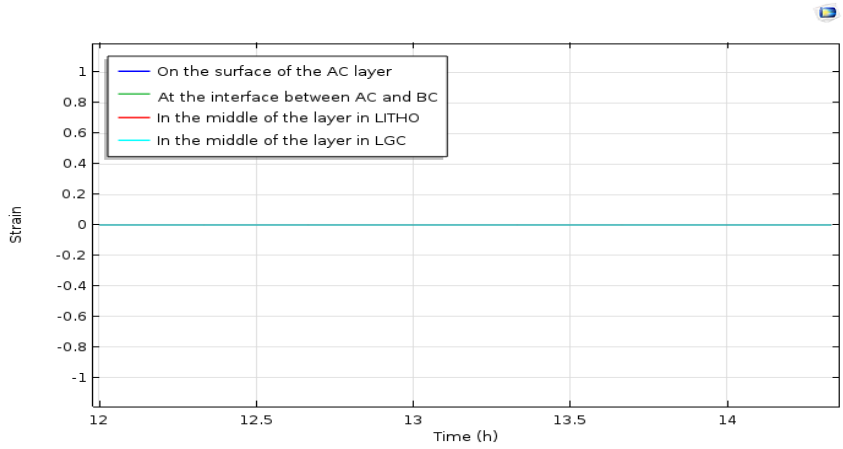

Fig. 8.b Temporal distribution of longitudinal deformations in the different layers of NR4 during a rainfall of maximum intensity of 53.06 mm/h

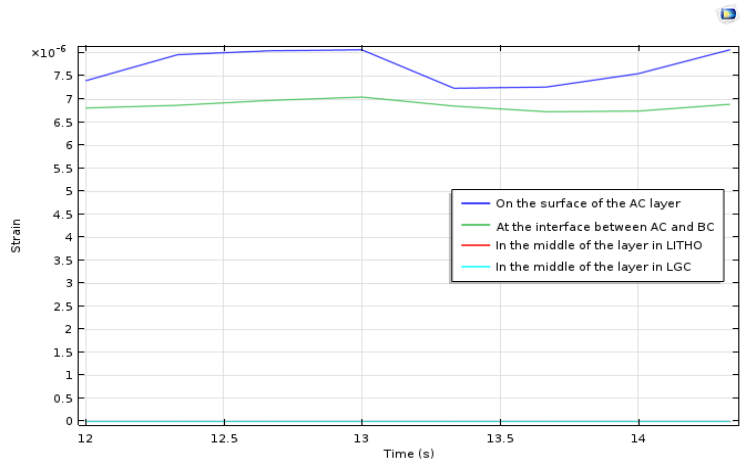

Fig. 8.c Temporal distribution of deformations according to depth in the different layers of NR4 during a shower of maximum intensity of 99 mm/h

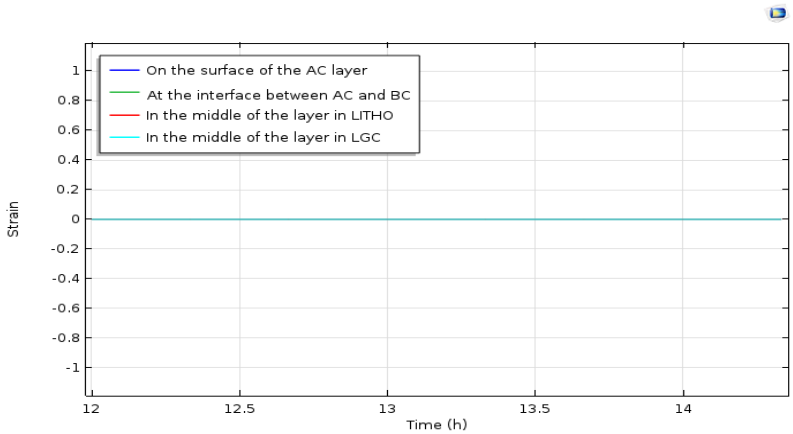

Fig. 8.d Temporal distribution of longitudinal deformations in the different layers of NR4 during a rainfall of maximum intensity of 99 mm/h

Table 7. Maximum simulated deformations in the pavement for a rainfall of 53.06 mm/h with a frequency of occurrence Tr of 2 years. ε_{xx} and ε_{zz} are respectively the longitudinal deformations and the deformations along the depth of the pavement

Pavement	ε_{xx}	ε_{zz}	LOG (ε_{xx})	LOG (ε_{zz})
NR2	$1.6\ 10^{-8}$	$8.3\ 10^{-6}$	-7.8	-5.1
NR2	0	$7\ 10^{-6}$	-	-5.2
NR4	0	$8.2\ 10^{-6}$	-	-5.1
NR4	0	$7.1\ 10^{-6}$	-	-5.1

Table 8. Maximum simulated deformations in the pavement for a rainfall of 99 mm/h with a frequency of occurrence Tr of 15 years. ε_{xx} and ε_{zz} are respectively the longitudinal deformations and the deformations along the depth of the pavement

Pavement	ε_{xx}	ε_{zz}	LOG (ε_{xx})	LOG (ε_{zz})
NR2	$8.2\ 10^{-6}$	$8.2\ 10^{-6}$	-5.1	-5.1
NR2	$7.2\ 10^{-6}$	$7\ 10^{-6}$	-5.1	-5.2
NR4	0	$8.2\ 10^{-6}$	-	-5.1
NR4	0	$7.1\ 10^{-6}$	-	-5.1

The work of Kertesz et al. [6] showed that during rainy periods of about 8 minutes (short duration showers), the AC surface temperature is lower than that of the BC. This could be related to the fact that latent heat exchange is greater than sensible heat exchange when rainfall is longer.

While the temperature difference between AC and BC is constant during the first hour of rain, it varies in the following hours due to the greater sensitivity of AC to rain. Analysis of the above graphs of pavement surface temperatures indicates that the rain event results in lower temperatures and thus cooling of the pavement surface layer's AC and BC (Figs. 6.a, 6.b, 6.c, 6.d). The maximum rain intensity corresponds to the simulated minimum pavement surface layer's temperatures.

3.2 Thermomechanical Deformations of the Pavement Associated with a Rainy Event

The maximum rainfall (53.06 mm/h and 99 mm/h) intensity corresponds to the lowest temperature simulated on the pavement. The minimum deformations observed in the different layers correspond to this peak of rain intensity (t=26500s, i.e. about 13h21min30s**).** The cooling of the pavement reduces the deformations in the surface layers of the pavement **(**Figs. 7.a, 7.b, 7.c, 7.d).

The same observation is made in the lower pavement layers **(**Figs 8.a, 8.b, 8.c, 8.d**).** The deformations become more significant after the rain event. This means that the cooling phenomenon is over and the pavement continues its natural warming phenomenon related to the meteorological conditions due to solar radiation, the outside air temperature and the wind speed incident on its surface.

The logarithmic values of the maximum values of the deformations recorded in tables 8 and 9 were calculated and plotted in the classification diagram of the deformations of asphalt mixes [38]. The latter indicates that these hygro-thermomechanical deformations obtained are linear elastic and therefore reversible. These deformations were also compared to the eligibility thresholds for the design of T2 trafic pavements [39]. They are also below the admissibility thresholds. When compared to the maximum deformations obtained during a heat wave [30], they are of the same order of magnitude and 10 to 1000 times less important depending on the depth and length of the pavement. Under the weather conditions and with the assumptions of impermeability of the layers, rainfall would reduce the risk of permanent deformations as demonstrated by the work of Wang et al. [37].

4. CONCLUSION

The objective of the study is to numerically evaluate the hygrothermomechanical deformations of pavements subjected to heavy rainfall in the hot and dry tropical climate of the city of Ouagadougou. Temperature profiles indicating pavement cooling during the rainy episode and generating reversible hygrothermomechanical deformations were observed.The resulting maximum deformations are acceptable for a T2 trafic pavement design. The rains of minimum and maximum intensity observable in Burkina Faso, the frequencies of which are 2 years and 15 years for the two types of bituminous mixes studied, do not generate permanent thermomechanical deformations that could lead to the degradation of the pavements studied. In addition, the study highlighted the difference in rheological behavior observed between mixtures formulated with pure grade 35/50 bitumen and grade 10/65 modified bitumen as a function of the maximum rain intensity. However, a study considering the phenomena of water infiltration and runoff in the pavement layers could be considered to explain the deterioration observed in the rainy season.

ACKNOWLEDGEMENTS

We would like to thank the National Laboratory of Building and Public Works of Burkina Faso for its material and technical support. Our thanks also go to the National Directorate of Meteorology of Burkina Faso and Mister ZAI Oumar hydraulic engineer for its orientations.

COMPETING INTERESTS

Authors have declared that no competing interests exist.

REFERENCES

1. Yavuzturk C, Ksaibati K. Assessment of temperature fluctuations in asphalt pavements due to thermal environmental conditions using a two-dimensional, transient finite difference approach.

Research Rep. No. MPC 02-136, Mountain Plains Consortium; 2005.
2. Chiasson AD, Yavuzturk C, Ksaibati K. Linearized Approach for Predicting Thermal Stresses in Asphalt Pavements due to Environmental Conditions. Materials Civil Engineering. 2008;20:118–27.
3. Van Buren MA, Watt WE, Marsalek J, Anderson B. Thermal enhancement of stormwater runoff by paved surfaces. Water Research. 2000;34(4);1359–1371.
4. Janke BD, HerbW R, Mohseni O, Stefan H. G.Simulation of heat export by rainfall-runoff from a paved surface. Journal of Hydrology. 2009;365(3–4):195–212.
5. Cohard JM, Rosant JM, Rodriguez F, Andrieu H, mestayer PG, Guillevic P. Energy and water budgets of asphalt concrete pavement under simulated rain events. Urban Climate; 2017.
6. Kertesz R, SAnsalone J. Hydrologic Transport of Thermal Energy from Pavement.—Journal of Environmental Engineering. 2014;140(8):4014028.
7. Herb W, Velasquez R, Heinz Stefan, Mihai O, Marasteanu, Tim C. Simulation and Characterization of Asphalt Pavement Temperatures. Road Materials and Pavement Design. 2009;10(1): 233-247.
8. Kim K, Thompson AM, Botter G. Modeling of thermal runoff response from an asphalt-paved plot in the framework of the mass response functions. Water Resources Research. 2008;44(11):1–13.
9. Sansalone JJ, Teng Z. Transient rainfall-runoff loadings to a partial exfiltration system: Implications for urban water quantity and quality. Journal of Environmental Engineering-Asce. 2005; 131(8):1155–1167.
10. Thompson MR, Dempsey BJ, Hill H, Vogel H. Characterizing Temperature Effects for Pavement Analysis and Design. In: Transportation Research Record: Journal of the Transportation Research Board, No. 1121, Transportation Research Board of the National Academies, Washington, DC. 1987;14–22.
11. Omidvar H, Song J, Yang J, Arwatz G, Wang Z-H, Hultmark M., Kaloush K. Rapid Modification of Urban Land Surface Temperature during Rainfall. Department of Civil and Environmental Engineering, Princeton University, Princeton, NJ;2018.
12. Huang K, Shi X, Zollinger D, Mirsayar M, Wang A, Mo L. Use of MgO expansion agent to compensate concrete shrinkage in jointed reinforced concrete pavement under high-altitude environmental conditions, Constr. Build. Mater. 2019;202: 528–536.
13. Lyu Z, Yinchuan Guo Y, Zhihui Chen Z, Shen A, Qin X, Jingyu Y, Zhao M, Wang Z. Research on shrinkage development and fracture properties of internal curing pavement concrete based on humidity compensation. Construction and Building Materials. 2019;203:417–431.
14. Yousefieh N, Joshaghani A, Hajibandeh E, Shekarchi M. Influence of fibers on drying shrinkage in restrained concrete, Constr. Build. Mater. 2017;148:833–845.
15. Angel Mateos A, Harvey J, Bolander J, Wu R, Paniagua J, Paniagua F. Structural response of concrete pavement slabs under hygrothermal actions. Construction and Building Materials. 2020; 243:118261.
16. Lompo P. Les Matériaux Utilisés En Construction Routière En Haute-Volta. Un Matériau Non Traditionnel.Le Lithostab. Irf Ive Conference Routiere Africaine 20-25 Janvier Nairobi. Kenya. 1980:29-40.
17. Bourier R. Hydraulique appliquée. Le moniteur, ISBN 978-2-281-14204-4. 2018 ;127.
18. Desbordes M. Contribution à l'analyse et à la modélisation des mécanismes hydrologiques en milieu urbain. Thèse doctorat d'Etat, université des Sciences et Technologies du Languedoc, Montpellier.242 p. 1987.
19. Sighomnou D., Desbordes M. Recherche d'un modèle de pluie de projet adapté aux pré cipitations de la zone tropicale africaine ; Cas d'Adiopodoumé -Abidjan (Côte d'Ivoire). Hydrologie Continentale, n°2. 1988 ;131-139.
20. Asfour S. Récupération d'énergie dans les chaussées pour leur maintien hors gel. Phd Thesis. Université Blaise Pascal Clermont. 2017;115:262.
21. Hall MR, Dehdezi PK, Dawson AR, Grenfell J, Isola R. Influence of the thermophysical properties of pavement materials on the evolution of temperature depth profiles in different climatic regions. Journal Of Materials In Civil Engineering. 2012;24:32–47.
22. Sheeba JB, Rohini AK. Structural And Thermal Analysis Of Asphalt Solar Collector Using Finite Element Method. Journal Of Energy; 2014.

23. Aubinet M. Longwave sky radiation parameterizations. Solar Energy. 1994;53:147- 154.
24. Solaimanian M, Kennedy TW. Predicting Maximum Pavement Surface Temperature Using Maximum Air Temperature And Hourly Solar Radiation. Transportation Research Record. Journal Of The Transportation Research Board. 1993; 1417:1–11.
25. Morris MD. Factorial sampling plans for preliminary computational experiments. Technometrics. 1991;33(2):161-174. 36.
26. Ashrae. Ashrae handbook, fundamentals. American Society of Heating, Refrigerating and Air. Conditioning Engineers, Inc., Atlanta; 2001.
27. Di Benedetto H, Neifar M. Coefficients de dilatation et de contraction thermiques d'un Enrobé bitumineux avec et sans chargement Mécanique. Mechanical Tests For Bituminous Materials. Proceeding Of The 5th International Rilem Symposium. 1997:421-428..
28. Lewis RW, Nithiarasu P, Seetaramu KN. Fundamentals of the Finite Element method for Heat and Fluid Flow.John Wiley& Sons, Ltd; 2004.
29. Comsol tutorial. Introduction to Comsol Multiphysics. 2015;5(2).
30. Koudougou SM, Toguyeni DYK. Modeling of pavement behavior in tropical hot and dry conditions : Numerical Approach And Comparison On Road Section. Journal of materials science & surface engineering. 2020;7(1):919-927.
31. Carslaw MS, Jaeger JC, Conduction Of Heat In Solids.Oxford Science Publications; 1954.
32. Maher. A.. Bennert. T. A. Evaluation Of Poisson's Ratio For Use In The Mechanistic Empirical Pavement Design Guide (Mepdg); 2008.
33. Mirza MW. Development of Relationships To Predict Poisson's Ratio For Paving Materials. University Of Maryland. College Park. Md. Interteam Technical Report For Nchrp. 1999;1-37a..
34. Koudougou S, Tubreoumya G, Toguyeni D., Zaida, T. Experimental Alternative to the Determination of the Thermal Dependence of the Complex Modulus of Asphalt Mixes in Dry Tropical Areas. Journal of Minerals and Materials Characterization and Engineering. 2022;10:275-286.
35. Olard F.Comportement thermomécanique des enrobés bitumineux à basses températures. relations entre les propriétés du liant et de l'enrobé. Phd Thesis. Institut National Des Sciences Appliquées de Lyon. 2003;138.
36. Kim K, Thompson AM, Botter G. Modeling of thermal runoff response from an asphalt-paved plotin the framework of the mass response functions. Water Resources Research. 2008;44. DOI:10.1029/2007wr005993
37. Wang X, Gu X, Ni F, Deng H, Dong Q. Rutting resistance of porous asphalt mixture under coupled conditions of high temperature and rainfall. Construction and Building Materials. 2018;174:293–301.
38. Di Benedetto H. Nouvelle approche du comportement des enrobés bitumineux: résultats expérimentaux et formulation rhéologique, Mechanical Tests for Bituminous Mixes, Characterization, Design and Quality Control, Proceedings of the Fourth Rilem Symposium; 1990.
39. Lcpc-setra, Vin P. Conception et dimensionnement des structures de chaussée. Guide technique, Paris; 1994.

Peer-review history:
The peer review history for this paper can be accessed here:
https://www.sdiarticle5.com/review-history/91284